

Unique first-forbidden β -decay rates for neutron-rich nickel isotopes in stellar environment

Jameel-Un Nabi ¹ • Sabin Stoica

Abstract In astrophysical environments, allowed Gamow-Teller (GT) transitions are important, particularly for β -decay rates in presupernova evolution of massive stars, since they contribute to the fine-tuning of the lepton-to-baryon content of the stellar matter prior to and during the collapse of a heavy star. In environments where GT transitions are unfavored, first-forbidden transitions become important especially in medium heavy and heavy nuclei. Particularly in case of neutron-rich nuclei, first-forbidden transitions are favored primarily due to the phase-space amplification for these transitions. In this work the total β -decay half-lives and the unique first-forbidden(U1F) β -decay rates for a number of neutron-rich nickel isotopes, $^{72-78}\text{Ni}$, are calculated using the proton-neutron quasi-particle random phase approximation (pn-QRPA) theory in stellar environment for the first time. For the calculation of the β -decay half-lives both allowed and unique first-forbidden transitions were considered. Comparison of the total half-lives is made with measurements and other theoretical calculations where it was found that the pn-QRPA results are in better agreement with experiments and at the same time are suggestive of inclusion of rank 0 and rank 1 operators in first-forbidden rates for still better results.

Keywords beta decay rates, Gamow-Teller transitions, unique first forbidden transitions, pn-QRPA theory; strength distributions, r -process.

Jameel-Un Nabi

Faculty of Engineering Sciences, GIK Institute of Engineering Sciences and Technology, Topi 23640, Swabi, Khyber Pakhtunkhwa, Pakistan

Sabin Stoica

Horia Hulubei Foundation, P. O. Box MG-12, 071225, Magurele, Romania

¹Corresponding author email : jameel@giki.edu.pk

Introduction

Reliable and precise knowledge of the β -decay for neutron-rich nuclei is crucial to an understanding of the r -process. Both the element distribution on the r -path, and the resulting final distribution of stable elements are highly sensitive to the β -decay properties of the neutron-rich nuclei involved in the process (1; 2). There are about 6000 nuclei between the β stability line and the neutron drip line. Most of these nuclei cannot be produced in terrestrial laboratories and one has to rely on theoretical extrapolations for beta decay properties. In neutron-rich environments electron neutrino captures could not only amplify the effect of β -decays but the subsequent ν -induced neutron spallation can also contribute towards changing the r -abundance distribution pattern (3). Correspondingly reliable predictions of β -decay for neutron-rich nuclei are considered to be very important for r -process nucleosynthesis.

The weak interaction rates are the important ingredients playing a crucial role in practically all stellar processes: the hydrostatic burning of massive stars, presupernova evolution of massive stars, and nucleosynthesis (s-, p-, r-, rp-) processes (see, for example, the seminal paper by Burbidge and collaborators (4)). For densities $\rho \lesssim 10^{11} \text{g/cm}^3$, stellar weak interaction processes are dominated by Gamow-Teller (GT) and, if applicable, by Fermi transitions. For nuclei lying in the vicinity of the line of stability, forbidden transitions contribute sizably for $\rho \gtrsim 10^{11} \text{g/cm}^3$ when the electron chemical potential reaches values of the order of 30 MeV or more (5).

During presupernova stage of stellar evolution, electron capture dominates the weak interaction processes. However, after silicon depletion in the core and during the silicon shell burning, β -decay competes temporarily with electron capture and further cools the star. Unlike electron capture, the β -decay at silicon burning stage

increases and this bears consequences because β -decays are additional neutrino source and add to the cooling of the stellar core and a reduction in stellar entropy. This cooling of stellar core can be quite efficient as often the average neutrino energy in the involved β -decays is larger than for the competing electron capture processes. Consequently, the β -decay lowers the stellar core temperature after silicon shell burning. For a discussion on the fine-tuning of lepton-to-baryon ratio of stellar matter during presupernova evolution see Ref. (6). As the density of the stellar core increases the allowed β -decay becomes unimportant and hindered due to the fact that the increasing Fermi energy of electrons blocks the available phase space for the electron to be produced in the β -decay. (For a detailed discussion of the role of weak interaction in the presupernova evolution of massive stars see Ref. (7).) In case of neutron-rich nuclei, first-forbidden β -decay may become important due to the enlarge phase space for these transitions (8; 9).

Reliable, quantitative estimates of β -decay half-lives of neutron-rich nuclei are needed in astrophysics for the understanding of supernova explosions, and the processes of nucleosynthesis, particularly the r -process. The β -decay half-lives are also needed for the experimental exploration of the nuclear landscape at existing and future radioactive ion-beam facilities. The calculation of β -decay half-lives in agreement with experimental results has been a challenging problem for nuclear theorists.

Because of the scarcity of experimental data, majority of the β -decay rates of the neutron-rich nuclei have been investigated using theoretical models. Several models of different level of sophistication for determining β -decay half-lives have been proposed and applied over the years. One can mention the more phenomenological treatments based on Gross Theory (e.g. (10)) as well as microscopic treatments that employ the proton-neutron quasiparticle random phase approximation (pn-QRPA) (11; 12) or the shell model (13). The later hybrid version of the RPA models developed by Möller and coworkers, combines the pn-QRPA model with the statistical Gross Theory of the first-forbidden decay (pnQRPA+ffGT)(14). There are also some models in which the ground state of the parent nucleus is described by the Hartree-Fock BCS method, or other density functional method (DF) and which use the continuum QRPA (CQRPA) (e.g. (15)). Recently relativistic pn-QRPA (RQRPA) models have been applied in the treatment of neutron-rich nuclei in the $N \sim 50$, $N \sim 82$ and $Z \sim 28$ and 50 regions (16; 17). Despite continuing improvements the predictive power of these conventional models is rather limited for β -decay half-lives of nuclei.

The microscopic calculations of allowed weak interaction rates using the pn-QRPA model (18; 11; 12) and unique first-forbidden (U1F) β -decay properties by Homma and collaborators (19), under terrestrial conditions, led to a better understanding of the r -process. It was shown in Ref. (19) that a larger contribution to the total transition probability for near-stable and near-magic nuclei came from U1F transitions (see Fig. 9 and Table IX of (19)). According to the β -decay studies by Borzov (20), the allowed β -decay approximation alone is not adequate to describe the isotopic dependence of the β -decay characteristics, specially for the nuclei crossing the closed N and Z shells and forbidden transitions give a dominant contribution to the total half-life for nuclei crossing the closed shells, specially for $N < 50$ in ^{78}Ni region. Recently large-scale shell-model calculation of the half-lives, including first-forbidden contributions, for r -process waiting-point nuclei was also performed (21). However there was a need to go to domains of high temperature and density scales where the weak interaction rates are of decisive importance in studies of the stellar evolution (see e.g. (20)). Moving on from terrestrial to stellar domain one notes two microscopic approaches, namely the shell model (22) and the pn-QRPA (23), have so far been successfully used in the large-scale calculation of stellar weak-interaction mediated rates for r -process applications. Whereas the advantage of the shell model clearly lies in it's ability to take into account the detailed structure of the β -strength functions, the shell model is forced to use approximations like Brink's hypothesis (in electron capture direction) and back resonances (in β -decay direction) when extending the calculation to high-lying parent excited states which can contribute rather significantly to the total weak rate in stellar environment. Brink's hypothesis states that GT strength distribution on excited states is *identical* to that from ground state, shifted *only* by the excitation energy of the state. GT back resonances are the states reached by the strong GT transitions in the inverse process (electron capture) built on ground and excited states. The pn-QRPA model, on the other hand, gets rid of such approximations and allows a state-by-state evaluation of the weak rates by summing over Boltzmann-weighted, microscopically determined GT strengths *for all* parent excited states.

The recent measurement of the GT_+ strength distribution of ^{76}Se (24) supports the argument that, due to nuclear correlations across the $N = 40$ shell gap, the GT transitions for fp-nuclei with proton numbers $Z < 40$ and neutron numbers $N > 40$ would not be Pauli blocked. Nevertheless for neutron-rich nuclei U1F transitions are favored due to the amplification

of available phase space. Further in the large-scale shell-model first-forbidden calculation of Zhi and collaborators (21) the authors note that for $N = 50$ nuclei with $Z \geq 28$, contributions to the first forbidden transitions are nearly exclusively due to rank 2 operators. In this paper we attempt to calculate the allowed as well as the unique first-forbidden (U1F) β -decay rates for neutron-rich nickel isotopes ($^{72-78}\text{Ni}$) using the pn-QRPA model. Further the calculations are extended from terrestrial to stellar domain for the first time using the pn-QRPA theory. Motivation of the current work was primarily based on the comments given by Homma and collaborators that the U1F transition has large enough contribution to the total transition probability and inclusion of U1F transition greatly improves the calculated half-lives using the pn-QRPA model (19). It is worthwhile to also study the effects of non-unique forbidden transitions which are expected, for some nuclei, to have still larger contribution to the calculated half-lives (as also mentioned in (19)). We would like to include this desired modification in our nuclear code as a future project. The theory of allowed and first-forbidden β -decay transitions (along with its leptonic phase-space content and nuclear matrix elements) is well-established (25; 26; 27; 28; 29). Whereas the allowed β -decay (having the same parity before and after the decay) is relatively simple to calculate, the first-forbidden decay shows a far wider spectrum both in lepton kinematics and in nuclear matrix elements (26; 25; 29).

The pn-QRPA formalism for calculations of the total β -decay half-lives and U1F β -decay rates for neutron-rich nickel isotopes are discussed in Section 2. Results and comparisons with experimental and other theoretical calculation are shown in Section 3. Section 4 outlines the importance of the results in connection with the simulation of the advanced stages of stellar evolution and heavy element nucleosynthesis and concludes our discussion on consequences of U1F β -decays in stellar matter.

2 Formalism

In the pn-QRPA formalism (30), proton-neutron residual interactions occur in two different forms, namely as particle-hole (ph) and particle-particle (pp) interactions. The particle-hole and particle-particle interactions can be given a separable form because β^- transitions are dominated by the particle-hole interaction. These ph and pp forces are repulsive and attractive, respectively, when the strength parameters χ for ph GT force and κ for pp GT force take positive values. The

advantage of using these separable GT forces is that the QRPA matrix equation reduces to an algebraic equation of fourth order, which is much easier to solve as compare to full diagonalization of the non-Hermitian matrix of large dimensionality (30; 19).

Essentially we first construct a quasiparticle basis (defined by a Bogoliubov transformation) with a pairing interaction, and then solve the RPA equation with a schematic separable GT residual interaction. The single particle energies were calculated using a deformed Nilsson oscillator potential with a quadratic deformation. The pairing correlation was taken into account in the BCS approximation using constant pairing forces. The BCS calculation was performed in the deformed Nilsson basis for neutrons and protons separately. The formalism for calculation of allowed β -decay rates in stellar matter using the pn-QRPA model can be seen in detail from Refs. (31; 23). Below we describe briefly the necessary formalism to calculate the U1F β -decay rates.

Allowed Fermi and GT transitions have a maximum spin change of one unit and no change in parity of the wavefunction. In contrast, the most frequent occurrence of a forbidden decay is when the initial and final states have opposite parities, and thus the selection rule for allowed decay is violated. The spins of the initial and final states can be different at most by $\Delta J = 0, \pm 1, \pm 2$ for the first-forbidden transitions (those transitions for which $\Delta J^\pi = 2^-$ are termed as unique first-forbidden). The isospin selection rule remains the same as for allowed decays. For the calculation of the U1F β -decay rates, nuclear matrix elements of the separable forces which appear in RPA equation are given by

$$V_{pn,p'n'}^{ph} = +2\chi f_{pn}(\mu) f_{p'n'}(\mu), \quad (1)$$

$$V_{pn,p'n'}^{pp} = -2\kappa f_{pn}(\mu) f_{p'n'}(\mu), \quad (2)$$

where

$$f_{pn}(\mu) = \langle j_p m_p | t_{-r} [\sigma Y_1]_{2\mu} | j_n m_n \rangle \quad (3)$$

is a single-particle U1F transition amplitude (the symbols have their normal meaning). Note that μ takes the values $\mu = 0, \pm 1$, and ± 2 (for allowed decay rates μ only takes the values 0 and ± 1), and the proton and neutron states have opposite parities (19). For the sake of consistency we chose to keep the same values of interaction constants ($\chi = 0.35$ MeV and $\kappa = 0.001$ MeV for allowed and $\chi = 0.35$ MeV fm $^{-2}$ and $\kappa = 0.001$ MeV fm $^{-2}$ for U1F transitions). For choice of strength of interaction constants in the pn-QRPA model we refer to (11; 12; 19).

Deformations of the nuclei were calculated using

$$\delta = \frac{125(Q_2)}{1.44(Z)(A)^{2/3}}, \quad (4)$$

where Z and A are the atomic and mass numbers, respectively and Q_2 is the electric quadrupole moment taken from Ref. (32). Q-values were taken from the recent mass compilation of Audi et al. (33).

The U1F β -decay rates from the i th state of the parent to the j th state of the daughter nucleus is given by

$$\lambda_{ij} = \frac{m_e^5 c^4}{2\pi^3 \hbar^7} \sum_{\Delta J^\pi} g^2 f(\Delta J^\pi; ij) B(\Delta J^\pi; ij), \quad (5)$$

where $f(\Delta J^\pi; ij)$ and $B(\Delta J^\pi; ij)$ are the integrated Fermi function and the reduced transition probability, respectively, for the transition $i \rightarrow j$ which induces a spin-parity change ΔJ^π and g is the weak coupling constant which takes the value g_V or g_A according to whether the ΔJ^π transition is associated with the vector or axial-vector weak-interaction. The phase-space factors $f(\Delta J^\pi; ij)$ are given as integrals over the lepton distribution functions and hence are sensitive functions of the temperature and density in stellar interior. The $B(\Delta J^\pi; ij)$ are related to the U1F weak interaction matrix elements stated earlier.

For the first-forbidden transitions the integral can be obtained as

$$f = \int_1^{w_m} w \sqrt{w^2 - 1} (w_m - w)^2 [(w_m - w)^2 F_1(Z, w) + (w^2 - 1) F_2(Z, w)] (1 - G_-) dw, \quad (6)$$

where w is the total kinetic energy of the electron including its rest mass and w_m is the total β -decay energy ($w_m = m_p - m_d + E_i - E_j$, where m_p and E_i are mass and excitation energies of the parent nucleus, and m_d and E_j of the daughter nucleus, respectively). G_- are the electron distribution functions. Assuming that the electrons are not in a bound state, these are the Fermi-Dirac distribution functions,

$$G_- = [\exp(\frac{E - E_f}{kT}) + 1]^{-1}. \quad (7)$$

Here $E = (w - 1)$ is the kinetic energy of the electrons, E_f is the Fermi energy of the electrons, T is the temperature, and k is the Boltzmann constant.

The Fermi functions, $F_1(\pm Z, w)$ and $F_2(\pm Z, w)$ appearing in Eq. (6) are calculated according to the procedure adopted by Gove and Martin (34).

The number density of electrons associated with protons and nuclei is $\rho Y_e N_A$, where ρ is the baryon density, Y_e is the ratio of electron number to the baryon number, and N_A is the Avogadro's number.

$$\rho Y_e = \frac{1}{\pi^2 N_A} \left(\frac{m_e c}{\hbar}\right)^3 \int_0^\infty (G_- - G_+) p^2 dp, \quad (8)$$

where $p = (w^2 - 1)^{1/2}$ is the electron or positron momentum, and Eq. (8) has the units of *moles cm*⁻³. G_+ are the positron distribution functions given by

$$G_+ = \left[\exp\left(\frac{E + 2 + E_f}{kT}\right) + 1 \right]^{-1}. \quad (9)$$

Eq. (8) is used for an iterative calculation of Fermi energies for selected values of ρY_e and T .

There is a finite probability of occupation of parent excited states in the stellar environment as a result of the high temperature in the interior of massive stars. Weak decay rates then also have a finite contribution from these excited states. The occupation probability of a state i is calculated on the assumption of thermal equilibrium,

$$P_i = \frac{\exp(-E_i/kT)}{\sum_{i=1} \exp(-E_i/kT)}, \quad (10)$$

where E_i is the excitation energy of the state i , respectively. The rate per unit time per nucleus for any weak process is then given by

$$\lambda = \sum_{ij} P_i \lambda_{ij}. \quad (11)$$

The summation over all initial and final states are carried out until satisfactory convergence in the rate calculations is achieved. We note that due to the availability of a huge model space (up to 7 major oscillator shells) convergence is easily achieved in our rate calculations for excitation energies well in excess of 10 MeV (for both parent and daughter states).

3 Results and comparison

In this section we present the phase space calculation, strength distributions calculation, total β -decay half-lives and total stellar β -decay rates for neutron-rich Ni isotopes. The calculated total terrestrial half-lives are also compared with the measured ones to estimate the accuracy of the model.

The phase space calculation for allowed and U1F transitions, as a function of stellar temperature and density, for the neutron-rich nickel isotopes are shown

in Tables 1 and 2. The phase space is calculated at selected density of 10^2 g/cm³, 10^6 g/cm³ and 10^{10} g/cm³ (corresponding to low, intermediate and high stellar densities, respectively) and stellar temperature $T_9 = 0.01, 1, 3$ and 10 (T_9 gives the stellar temperature in units of 10^9 K). Table 1 shows the result for $^{72-75}\text{Ni}$ whereas Table 2 displays the phase space calculation for $^{76-78}\text{Ni}$. It can be seen from these tables that for low and intermediate stellar densities the phase space increase by 2-5 orders of magnitude as the stellar temperature goes from $T_9 = 0.01$ to 1. Moreover the phase space remains same as stellar temperature rises from $T_9 = 1$ to 10. For high densities the phase space is essentially zero at $T_9 = 0.01$ and increases with increasing temperatures. As the stellar core becomes more and more dense the phase space decreases. For the case of $^{72-75}\text{Ni}$, the phase space increases by 1-2 orders of magnitude for U1F transitions as the stellar temperature and density increases. As the nickel isotopes becomes more and more neutron-rich, the phase space enhancement for U1F transitions decreases but still is bigger than the phase space for allowed transitions.

In order to ensure reliability of calculated β -decay rates, experimental (XUNDL) data were incorporated in the calculation wherever possible and the calculated excitation energies were replaced with measured levels when they were within 0.5 MeV of each other. Missing measured states were inserted and inverse transitions (along with their $\log ft$ values), where applicable, were also taken into account. No theoretical levels were replaced with the experimental ones beyond the excitation energy for which experimental compilations had no definite spin and/or parity. This recipe for incorporation of measured data is same as used in earlier pn-QRPA calculation of stellar weak rates (31; 23).

We present the calculated strength distributions of $^{72-78}\text{Ni}$, both due to allowed and U1F transitions in Fig. 1 and Fig. 2. Calculations for $^{72-74}\text{Ni}$ are displayed in Fig. 1 whereas Fig. 2 depicts result for $^{75-78}\text{Ni}$. All energies are given in units of MeV, allowed strengths are given in arbitrary units and U1F transitions are given in units of fm². In these figures we only show low-lying strength distribution up to an excitation energy of 2 MeV in daughter nucleus. Calculated values of strength smaller than 10^{-4} are not shown in these figures. For the case of ^{72}Ni , we show the 1^+ states as filled circles and 2^- states as open squares (Fig. 1). For the case of ^{73}Ni , no allowed GT transitions were calculated up to excitation energies of 2 MeV in ^{73}Cu and low-energy region is populated by U1F transitions. Same is the case for other odd-A isotopes of nickel, ^{75}Ni and ^{77}Ni (Fig. 2). The excitation energy of 1^+ state is important for the evaluation of the transition rate in

^{78}Ni and bear consequences for r -process simulation as pointed out in a recent work by Minato and Bai (35). The effect of tensor force on β -decay rates was studied within the Hartree-Fock plus proton-neutron random phase approximation employing the Skyrme force in Ref. (35). The authors concluded that the tensor force makes dramatic improvement in the prediction of β -decay half-lives of the even-even magic (and semi-magic) nuclei where the effect of isoscalar pairing is negligible. It was further deduced that the tensor force had a significant contribution to the low-lying GT distribution, in particular, the effect of the tensor terms in the residual interaction of RPA was more important than the change of the spin-isospin splitting in the Hartree-Fock. Both Figs. 1 and 2 demonstrate the fact that U1F transitions play a crucial role in reducing the energy of the GT state (specially for the odd A nuclei) which in turn contribute to the reduction of calculated half-lives as discussed below.

For the Ni isotopic chain the results for terrestrial half-lives are shown in Fig. 3. We also compare our calculation with the experimental values (36; 37; 38) and with the self-consistent density functional + continuum quasiparticle random phase approximation (DF3 + CQRPA) calculation of Ref. (39). The pn-QRPA calculated half-lives including only allowed GT transitions are also shown in Fig. 3 to show the improvement brought by inclusion of U1F β -decay rates which results in calculation of smaller half-lives. Excellent agreement with measured half-lives is achieved when U1F transitions are included for the case of $^{74,75}\text{Ni}$. It is to be noted that Ref. (39) overestimate the total β -decay rates for $^{74,75}\text{Ni}$ roughly by a factor of two. The pn-QRPA half-lives are roughly a factor two bigger than experimental half-lives (36) for $^{72,73}\text{Ni}$ whereas the calculated half-lives of Ref. (39) are in better comparison with the corresponding measured values. For the remaining cases, $^{76-78}\text{Ni}$, the pn-QRPA calculated half-lives are again roughly a factor two bigger than the measured half-lives. The DF3 + CQRPA calculation of Ref. (39) are also 20% - 30% bigger than the measured half-lives for the case of $^{77-78}\text{Ni}$. The results are suggestive that possible inclusion of rank 0 and rank 1 operators in calculation of first-forbidden β -decay rates can bring further improvement in the overall comparison with the experimental data which we plan to incorporate in future. The incorporation of U1F transitions decreased the calculated half-lives from about 36% for the case of ^{72}Ni to about 47% for the case of ^{78}Ni . Fig. 3 proves that the inclusion of the U1F contribution makes the half-life predictions more reliable for neutron-rich nickel isotopes.

Recently a large-scale shell-model calculation of half-lives including first-forbidden transitions (including

rank 0, 1 and 2 operators) was performed for r -process waiting-point nuclei (21). In their work the authors remark that for $N = 50$ nuclei with $Z \geq 28$, contributions to the first forbidden transitions are nearly exclusively due to rank 2 operators. There the authors concluded that forbidden transitions have a small effect (reduction of 5% - 25%) on the half-lives of $N = 50$ waiting-point nuclei which is much smaller than the contributions from forbidden transitions calculated in this work. However there are at least three big differences in the shell model and the current pn-QRPA model calculations. Firstly, as mentioned previously, the current pn-QRPA model is not capable of calculating forbidden contributions of rank 0 and rank 1 operators which the shell model calculation can (it is remarked by the authors that for $Z < 28$ and $N = 50$, rank 0 and rank 1 operators contribute significantly to the first forbidden transitions). Secondly quenching was used in the shell model calculation and different quenching factors ranging from 0.38 to 1.266 was used for the various nuclear matrix elements. No explicit quenching factor was used in current calculation in contrast to shell model calculation. Last but not the least, due to model space limitation in shell model calculation, authors in Ref. (21) were not able to recover the full GT and first-forbidden strengths built on the ground and isomeric states. A completely converged calculation of the first-forbidden transition strength was not possible in shell model due to computational limitations (they used a Lanczos scheme with 100 iterations which was able to converge the states for excitation energies in the vicinity of only 2.5 MeV). The pn-QRPA model has no such computational limitations and convergence was achieved for excitation energies well in excess of 10 MeV. The UIF contribution in the current pn-QRPA model is well within the percentage contribution of first-forbidden transitions (to the total half-lives) as calculated by authors employing the FRDM + QRPA model in Ref. (14).

The UIF β -decay rates were calculated for densities in the range $10\text{-}10^{11}\text{g/cm}^3$ and temperature range $0.01 \leq T_9 \leq 30$. Figs. 4- 10 show three panels depicting pn-QRPA calculated allowed and UIF β -decay rates for temperature range $0.01 \leq T_9 \leq 30$ for the neutron-rich nickel isotopes. The upper panel depicts the situation at a low stellar density of 10^2 g/cm^3 , the middle panel for 10^6 g/cm^3 and the lower panel at a high stellar density of 10^{10} g/cm^3 . It is to be noted that for all figures the abscissa is given in logarithmic scales. Fig. 4 depicts stellar β -decay rates for ^{72}Ni in units of s^{-1} . It is pertinent to mention that contribution from all excited states are included in the final calculation of all decay rates. It can be seen from this figure that for low

and intermediate densities (10^2 and 10^6 g/cm^3) the β -decay rates (both allowed and UIF) remain almost the same as a function of stellar temperature. This feature remains the same for all following figures. At low temperatures ($T_9 \leq 5$) the UIF transition is roughly half the allowed transition (for phase space consideration refer to Table 1). At high stellar temperatures the allowed transitions become bigger by as much as a factor of 60 as more and more excited states contribute significantly to the allowed GT rates. At high stellar density (10^{10} g/cm^3) the β -decay rates tend to go down due to the blocking of the available phase space of increasingly degenerate electrons and one notes that allowed GT rates are tens of orders of magnitude bigger than UIF rates. As the stellar temperature rises, the orders of magnitude difference reduces and for $T_9 = 30$ the allowed rates are around two orders of magnitude bigger than UIF rates. At high densities and high temperatures the contribution to the total β -decay rates by the excited states is very important. The rates rise with higher temperature as more excited states start contributing when the temperature increases. Increasing temperature and density have opposite contributions to the calculated rates. Whereas growth of the stellar density suppresses the β decay rates due to a diminishing phase space available for escaping electrons, increase in temperature weakens the Pauli blocking and therefore enhances the contribution of the GT₋ transitions from excited states of the parent nucleus.

Fig. 5 shows the case of odd A nucleus ^{73}Ni . For low and intermediate stellar densities the allowed GT rates are bigger by a factor of 1.6 at $T_9 = 0.01$ to a factor of 42 at $T_9 = 30$. For high densities the allowed rates are a factor 90 bigger than the UIF rates at $T_9 = 30$. Due to a significantly larger number of available parent excited states in odd-A nuclei, the contributions from allowed and UIF rates increases with temperature when compared with the even-even isotopes. The results almost follow the same trend as shown in Fig. 4. The effects of increasing temperature and density on the decay rates were discussed earlier.

Fig. 6 shows the next even-even case of ^{74}Ni . Here one notes that at low and intermediate stellar densities and low temperatures ($T_9 \leq 5$) the allowed GT rates are only a factor of 1.2 bigger than UIF rates whereas at $T_9 = 30$ the allowed rates are a factor 18 bigger. For high densities the allowed rates are a factor 38 bigger than the UIF rates at a stellar temperature of $T_9 = 30$. Once again the results almost follow the same trend as shown in Fig. 4.

Similarly the allowed GT rates for ^{75}Ni are only a factor of 1.3 bigger than UIF rates for low temperatures ($T_9 \sim 0.2$) and low and intermediate stellar densities

(Fig. 7). As the stellar temperatures increases to $T_9 = 30$, the allowed rates are bigger by a factor of 20. For high densities and temperature the allowed rates are almost a factor 40 bigger.

Fig. 8 shows the case of ^{76}Ni and is very much similar to Fig. 6. At $T_9 = 30$ the enhancement in total β -decay rates, due to U1F contributions, is roughly double that for the case of ^{74}Ni (Fig. 6). Similarly Fig. 9 for ^{77}Ni is akin to Fig. 7. One notes that, for both even-even and odd-A isotopes of nickel, the U1F contributions increases as the number of neutrons increases. This is primarily because of the reduction in phase space of allowed β -decay rates as N increases.

Fig. 10 for ^{78}Ni (double-magic nucleus) is very much similar to the even-even case of ^{76}Ni (Fig. 8). The half-life of ^{78}Ni (and consequently its β -decay rate) is believed to set the processing timescale for the synthesis of elements beyond $A \sim 80$. The neutron separation energy shows discontinuity at $N = 50$ and consequently the r -process matter flow slows down. The β -decay of ^{78}Ni then takes charge and accordingly ^{78}Ni is considered to be a crucial waiting point nuclei for r -process. Fig. 10 shows that for stellar density range 10^2 - 10^6 g/cm^3 , the total β -decay rates of ^{78}Ni increase from 3.5 s^{-1} at $T_9 = 0.01$ to around 225 s^{-1} at $T_9 = 30$. As the stellar core stiffens to a density of around 10^{10} g/cm^3 , the β -decay rates decrease by tens of orders of magnitude at low stellar temperatures to around 67 s^{-1} at $T_9 = 30$. Further our calculation shows significant U1F contribution to total β -decay rates of ^{78}Ni at low stellar temperatures $T_9 \leq 1$. At high temperatures of $T_9 = 30$, the allowed rates are a factor 7 (for low and intermediate densities) to factor 13 bigger (for high densities) than the U1F β -decay rates.

It is to be noted that increasing the stellar temperature weakly affects the U1F β -decay rates. The reason is that the first-forbidden transitions are of relatively high energies and basically of the particle-hole nature. Therefore a smearing of single-particle strengths due to pairing correlations and temperature influence them considerably less. On the other hand the allowed GT rates increase at a faster pace with increasing temperature and hence explains this feature in all figures.

In the β -decay of a particular isotope, an emitted electron can receive any kinetic energy from zero up to the maximum kinetic energy available for the decay. In stellar environments, the electron density can be sufficiently high so that the low-energy states of the electron gas are essentially filled. In such an environment, there are fewer states available into which a low-energy electron can be emitted, and therefore β -decay is strongly inhibited if maximum kinetic energy available for the decay is small. For U1F decays, when maximum kinetic

energy available for the decay is small, the inhibition of unique first-forbidden decays is not as large as the inhibition of allowed, for the same temperature, density, and β -decay energy (39). This feature is also exhibited in all figures shown.

4 Conclusions

In this work the total stellar β^- -decay half-lives and U1F β -decay rates for a number of neutron-rich nuclei have been calculated, for the first time, using the pn-QRPA theory. The temperature and density profiles were relevant to advanced nuclear burning stages of the presupernova and supernova star. The results for total β -decay half-lives are in better agreement with the experimental results (36; 37; 38) as compared to the pn-QRPA calculated half-lives including only allowed GT transitions. At the same time the calculations suggest that incorporation of rank 0 and rank 1 operators in calculation of first-forbidden transitions can further improve the results and we plan to work on this in near future.

The microscopic calculation of U1F β -decay rates, presented in this work, could lead to a better understanding of the nuclear composition and Y_e in the core prior to collapse and collapse phase. The stellar β -decay rates of waiting point nucleus, ^{78}Ni , presented in this work can prove useful for r -process simulation which is a leading candidate for synthesizing heavy elements in astrophysical sites.

What possible implications can the enhanced U1F β -decay rates have for astrophysical scenarios? During the collapse phase allowed β -decays become unimportant due to the increased electron chemical potential which drastically reduces the phase space for the beta electrons. It is well known that a smaller lepton fraction disfavors the outward propagation of the post-bounce shock waves, as more overlying iron core has to be photo-dissociated. It is noted that the U1F β -decay rates yield higher Y_e in comparison to (only) allowed β -decay rates prior to collapse. This might assist the march of post-bounce shock for a successful supernova explosion to occur. Further these stronger β -decay rates can also assist in a more vigorous URCA process and may lead to cooler presupernova cores consisting of lesser neutron-rich matter than in presently assumed simulations. The reduced β -decay half-lives also bear consequences for site-independent r -process calculations and might result in speeding-up of the r -matter flow relative to calculations based on half-lives calculated from only allowed GT transitions. However studies on other neutron-rich isotopic chains including non-unique forbidden contributions, as well as

their relative abundance, are further required to draw more concrete conclusions and would be taken as a future assignment. Significant progress is expected, in part, to also come from next-generation radioactive ion-beam facilities (e.g. FAIR (Germany), FRIB (USA) and FRIB (Japan)) when we would have access to measured strength distribution of many more neutron-rich nuclei. The allowed and U1F β -decay rates on nickel isotopes were calculated on a fine temperature-density grid, suitable for simulation codes, and may be requested as ASCII files from the authors.

Acknowledgements The authors would like to acknowledge the support of the Horia Hulubei Foundation through the project PCE-IDEI-2011-3-0318, Contract no. 58.11.2011.

References

- Klapdor H. V.: The Shape of the beta strength function and consequences for nuclear physics and astrophysics. *Prog. Part. Nucl. Phys* **10**, 131 (1983).
- Grotz K. and Klapdor H. V.: *The Weak Interaction in Nuclear, Particle and Astrophysics*, Adam Hilger, Bristol, Philadelphia, New York, (1990).
- McLaughlin G. and Fuller G.: Weak Charge-changing Flow in Expanding r -process Environments. *Astrophys. J.* **489**, 766 (1997).
- Burbidge E. M., Burbidge G. R., Fowler W. A. and Hoyle F.: Synthesis of the elements in stars. *Rev. Mod. Phys.* **29**, 547 (1957).
- Cooperstein J and Wambach J.: Electron capture in stellar collapse. *Nucl. Phys. A* **420**, 591 (1984).
- Aufferdeide M. B., Fushiki I., Woosley S. E., Stanford E. and Hartmann D. H.: Search for important weak interaction nuclei in presupernova evolution. *Astrophys. J. Suppl. Ser.* **91**, 389 (1994).
- Langanke K and Martínez-Pinedo G.: Nuclear weak-interaction processes in stars. *Rev. Mod. Phys.* **75**, 819 (2003).
- Warburton E. K., Becker J. A., Millener D. J. and Brown B. A.: First-forbidden beta decay near $A = 40$. *Ann. Phys.* **187**, 471 (1988).
- Warburton E. K., Towner I. S. and Brown B. A.: First-forbidden β decay: Meson-exchange enhancement of the axial charge at $A \sim 16$. *Phys. Rev. C* **49**, 824 (1994).
- Takahashi K., Yamada M. and Kondoh T.: Beta-decay half-lives calculated on the gross theory. *At. Data Nucl. Data Tables* **12**, 101 (1973).
- Staudt A., Bender E., Muto K., Klapdor-Kleingrothaus H.V.: Second-Generation Microscopic Predictions of Beta-Decay Half-lives of Neutron-Rich Nuclei. *At. Data Nucl. Data Tables* **44**, 79 (1990)
- Hirsch M., Staudt A., Muto K., Klapdor-Kleingrothaus H.V.: Microscopic Predictions of β^+ /EC-Decay Half-Lives. *At. Data Nucl. Data Tables* **53**, 165 (1993)
- Muto K., Bender E. and Oda T.: β^+ decays of very proton-rich sd -shell nuclei. *Phys. Rev. C* **43**, 1487 (1991).
- Möller P., Pfeiffer B. and Kratz K.-L.: New calculations of gross β -decay properties for astrophysical applications: Speeding-up the classical r process. *Phys. Rev. C* **67**, 055802 (2003).
- Engel J., Bender M., Dobaczewski J., Nazarewicz W. and Surman R.: β decay rates of r -process waiting-point nuclei in a self-consistent approach. *Phys. Rev. C* **60**, 014302 (1999).
- Niksic T., Marketin T., Vretenar D., Paar N. and Ring P.: β -decay rates of r -process nuclei in the relativistic quasiparticle random phase approximation. *Phys. Rev. C* **71**, 014308 (2005).
- Marketin T., Vretenar D. and Ring P.: Calculation of β -decay rates in a relativistic model with momentum-dependent self-energies. *Phys. Rev. C* **75**, 024304 (2007).
- Klapdor H. V., Metzinger J. and Oda T.: Beta-decay half-lives of neutron-rich nuclei. *At. Data. Nucl. Data Tables* **31**, 81 (1984).
- Homma H., Bender E., Hirsch M., Muto K., Klapdor-Kleingrothaus H. V. and Oda T.: Systematic study of nuclear β decay. *Phys. Rev. C* **54**, 2972 (1996).
- Borzov I. N.: Beta-decay rates. *Nucl. Phys. A* **777**, 645, (2006).
- Zhi Q., Caurier E., Cuenca-García J. J., Langanke K., Martínez-Pinedo G. and Siega K.: Shell-model half-lives including first-forbidden contributions for r -process waiting point nuclei. *Phys. Rev. C*, **87**, 025803 (2013).
- Langanke K. and Martínez-Pinedo G.: Shell-Model calculations of stellar weak interaction rates: II. Weak rates for nuclei in the mass range $A = 45-65$ in supernovae environments. *Nucl. Phys. A* **673**, 481, (2000).
- Nabi J.-Un, Klapdor-Kleingrothaus H. V.: Microscopic calculations of stellar weak interaction rates and energy losses for fp- and fpq-shell nuclei. *At. Data Nucl. Data Tables* **88**, 237 (2004).
- Grewe E.-W. *et. al.*: The $(d, ^2\text{He})$ reaction on ^{76}Se and the double- β -decay matrix elements for $A=76$. *Phys. Rev. C* **78**, 044301 (2008).
- Schopper H. F.: *Weak Interactions and Nuclear Beta Decay*, North-Holland, Amsterdam (1966).
- Wu C. S. and Moszkowski S. A.: *Beta Decay*, Wiley, New York (1966).
- Commins E. D.: *Weak Interactions*, McGraw-Hill, New York (1973).
- Blatt J. M. and Weisskopf V. F.: *Theoretical Nuclear Physics*, Springer, Berlin (1979).
- Behrens H. and Bühring W.: *Electron Radial Wave Functions and Nuclear Beta-Decay*, Clarendon, Oxford (1982).
- Muto K., Bender E., Oda T. and Klapdor-Kleingrothaus H. V.: Proton-neutron quasiparticle RPA with separable Gamow-Teller forces. *Z. Phys. A* **341**, 407 (1992).
- Nabi J.-Un and Klapdor-Kleingrothaus H. V.: Weak Interaction Rates of sd -Shell Nuclei in Stellar Environments Calculated in the Proton-Neutron Quasiparticle Random-Phase Approximation. *At. Data Nucl. Data Tables* **71**, 149 (1999).
- Möller P. and Nix J. R.: Atomic mass and nuclear ground-state deformations calculated with a new macroscopic-microscopic model. *At. Data Nucl. Data Tables* **26**, 165 (1981).
- Audi G., Wapstra A. H. and Thibault C.: The AME2003 atomic mass evaluation (II). Tables, graphs and references. *Nucl. Phys. A* **729**, 337 (2003).
- Gove N. B. and Martin M. J.: Log-f tables for beta decay. *At. Data Nucl. Data Tables* **10**, 205 (1971).
- Minato F. and Bai C. L.: Impact of tensor force on β decay of magic and semimagic nuclei. *Phys. Rev. Lett.* **110**, 122501 (2013).
- Franchoo S. *et. al.*: Beta decay of $^{68-74}\text{Ni}$ and level structure of neutron-rich Cu isotopes. *Phys. Rev. Lett.* **81**, 3100 (1998).
- Ameil F. *et al.*: β decay half-lives of very neutron-rich isotopes of elements from Ti to Ni. *Eur. Phys. J. A* **1**, 275 (1998).
- Hosmer P. T. *et al.*: Half-life of the doubly magic r -process nucleus ^{78}Ni . *Phys. Rev. Lett.* **94**, 112501 (2005).
- Borzov I. N.: β -delayed neutron emission in the ^{78}Ni region. *Phys. Rev. C* **71**, 065801 (2005).

Table 1 Comparison of calculated allowed and unique first-forbidden (U1F) phase space factors for $^{72-75}\text{Ni}$ for different selected densities and temperatures in stellar matter. The first column gives stellar densities (ρY_e) having units of g/cm^3 , where ρ is the baryon density and Y_e is the ratio of the electron number to the baryon number. Temperatures (T_9) are given in units of 10^9 K.

ρY_e	T_9	Phase space (^{72}Ni)		Phase space (^{73}Ni)		Phase space (^{74}Ni)		Phase space (^{75}Ni)	
		Allowed	U1F	Allowed	U1F	Allowed	U1F	Allowed	U1F
10^2	0.01	1.7E+04	6.6E+04	9.5E+04	4.0E+05	8.1E+04	4.4E+05	4.0E+05	1.5E+06
	1	4.2E+08	1.1E+10	2.6E+08	1.1E+10	1.8E+08	7.2E+08	5.1E+08	1.4E+09
	3	4.2E+08	1.1E+10	2.6E+08	1.1E+10	1.8E+08	7.2E+08	5.1E+08	1.4E+09
	10	4.2E+08	1.1E+10	2.6E+08	1.1E+10	1.8E+08	7.2E+08	5.0E+08	1.4E+09
10^6	0.01	1.7E+04	6.6E+04	9.3E+04	3.9E+05	8.0E+04	4.4E+05	4.0E+05	1.5E+06
	1	4.2E+08	1.1E+10	2.6E+08	1.1E+10	1.8E+08	7.2E+08	5.1E+08	1.4E+09
	3	4.2E+08	1.1E+10	2.6E+08	1.1E+10	1.8E+08	7.2E+08	5.1E+08	1.4E+09
	10	4.2E+08	1.1E+10	2.6E+08	1.1E+10	1.8E+08	7.2E+08	5.0E+08	1.4E+09
10^{10}	0.01	0.0E+00	0.0E+00	0.0E+00	0.0E+00	0.0E+00	0.0E+00	0.0E+00	0.0E+00
	1	5.5E+07	2.5E+09	1.3E+07	5.3E+09	9.2E+06	2.0E+08	4.2E+07	5.6E+08
	3	5.6E+07	2.6E+09	1.3E+07	5.3E+09	9.7E+06	2.0E+08	4.3E+07	5.6E+08
	10	7.0E+07	3.0E+09	2.0E+07	5.5E+09	1.5E+07	2.3E+08	5.8E+07	3.5E+08

Table 2 Same as Table 1 but for $^{76-78}\text{Ni}$.

ρY_e	T_9	Phase space (^{76}Ni)		Phase space (^{77}Ni)		Phase space (^{78}Ni)	
		Allowed	U1F	Allowed	U1F	Allowed	U1F
10^2	0.01	1.9E+05	1.1E+06	4.3E+05	2.1E+06	3.4E+05	2.3E+06
	1	2.3E+08	3.2E+08	9.6E+08	1.3E+09	2.3E+08	4.0E+08
	3	2.3E+08	3.2E+08	9.6E+08	1.3E+09	2.3E+08	4.0E+08
	10	2.3E+08	3.1E+08	9.5E+08	1.3E+09	2.3E+08	4.0E+08
10^6	0.01	1.9E+05	1.1E+06	4.3E+05	2.1E+06	3.4E+05	2.3E+06
	1	2.3E+08	3.2E+08	9.6E+08	1.3E+09	2.3E+08	4.0E+08
	3	2.3E+08	3.2E+08	9.6E+08	1.3E+09	2.3E+08	4.0E+08
	10	2.3E+08	3.1E+08	9.5E+08	1.3E+09	2.3E+08	4.0E+08
10^{10}	0.01	0.0E+00	0.0E+00	0.0E+00	0.0E+00	0.0E+00	0.0E+00
	1	2.2E+07	6.8E+07	1.3E+08	5.4E+08	2.5E+07	5.5E+07
	3	2.3E+07	6.9E+07	1.4E+08	5.5E+08	2.5E+07	5.7E+07
	10	3.0E+07	8.1E+07	1.7E+08	5.7E+08	3.3E+07	7.1E+07

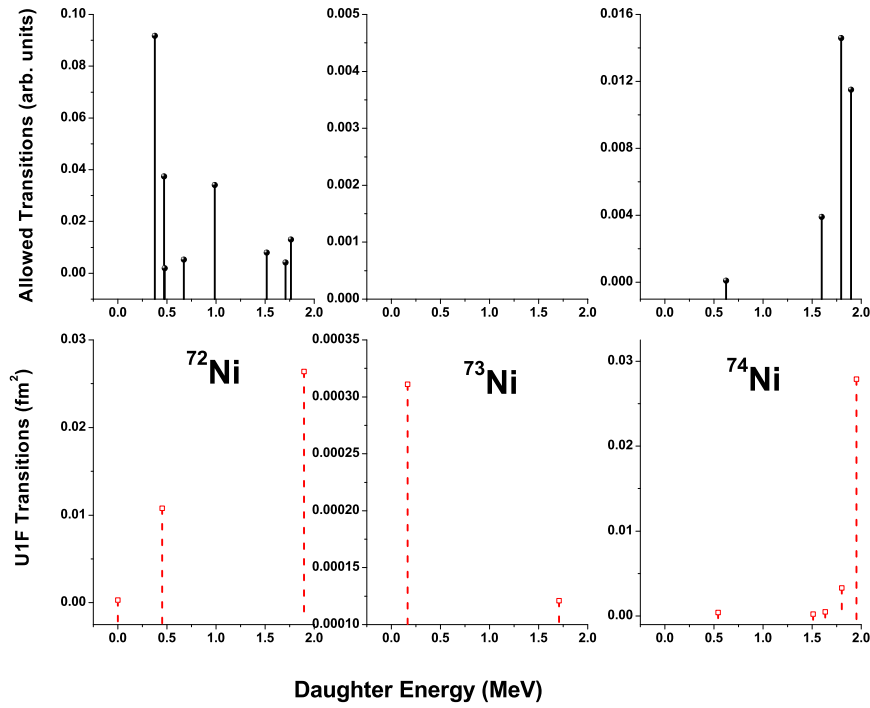


Fig. 1 Calculated strength distributions for allowed and U1F transitions for $^{72-74}\text{Ni}$.

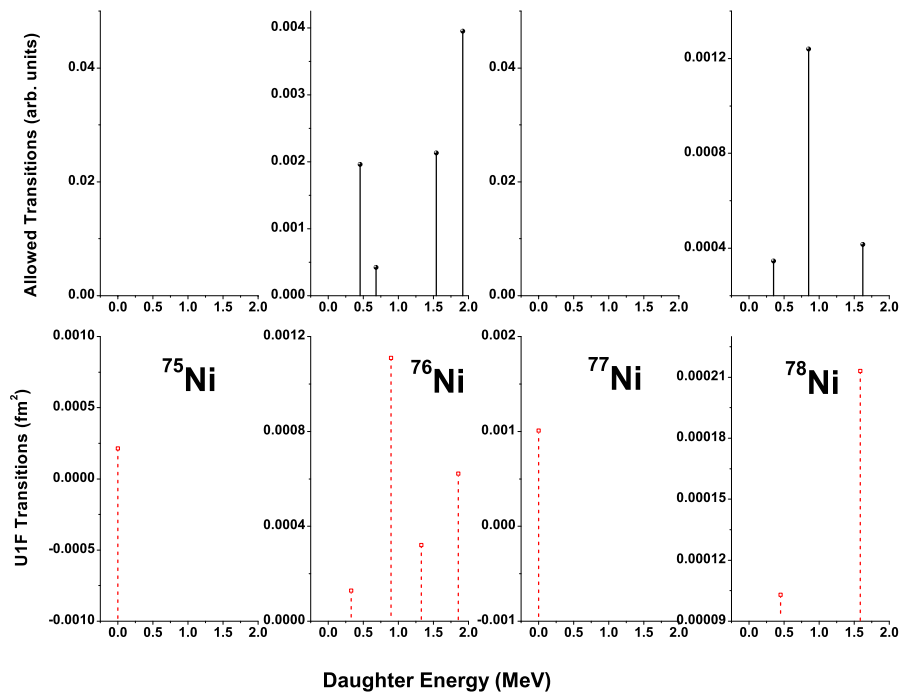


Fig. 2 Same as Fig. 1 but for $^{75-78}\text{Ni}$.

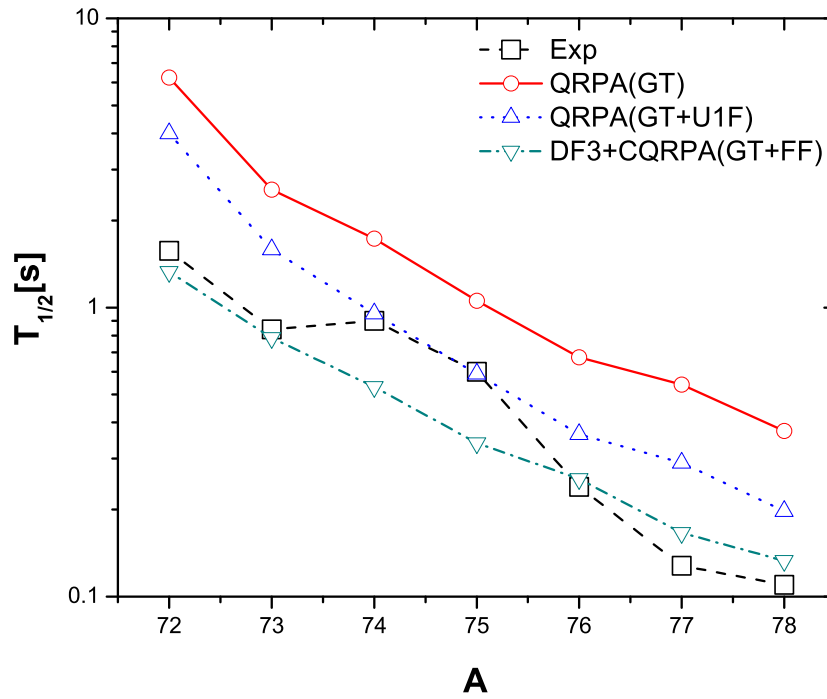


Fig. 3 Total β -decay half-lives for Ni isotopes calculated from the pn-QRPA (this work) including only the allowed (GT), allowed plus unique first-forbidden (GT+U1F) transitions, in comparison with the DF3+CQRPA (39) and experimental data (36; 37; 38).

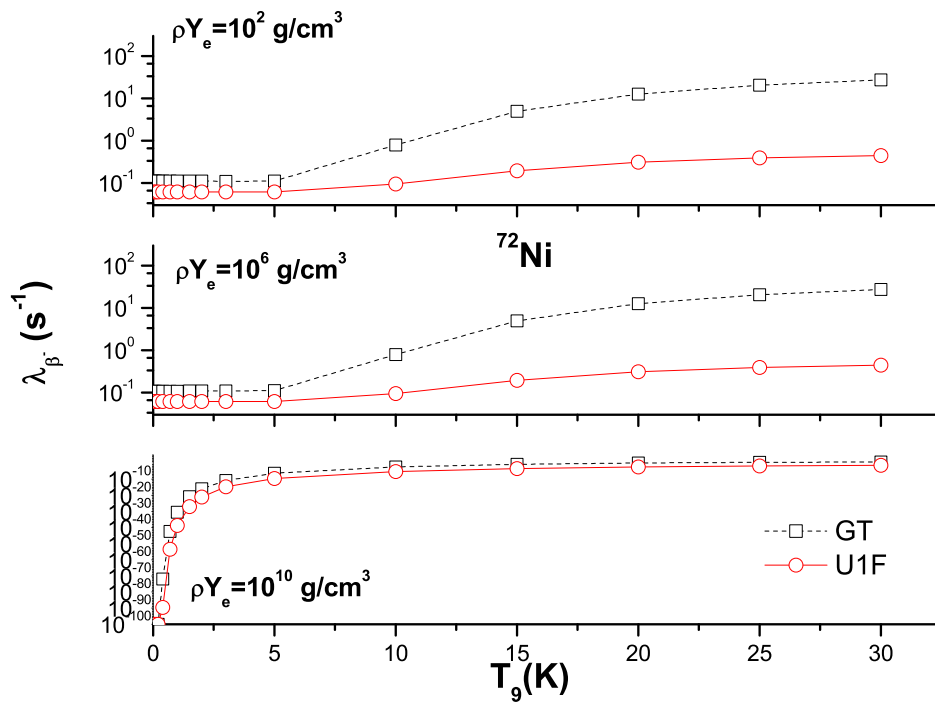


Fig. 4 Allowed (GT) and unique first-forbidden (U1F) β -decay rates on ^{72}Ni as function of temperature for different selected densities. All β decay rates are given in units of sec^{-1} . Temperatures (T_9) are given in units of 10^9 K.

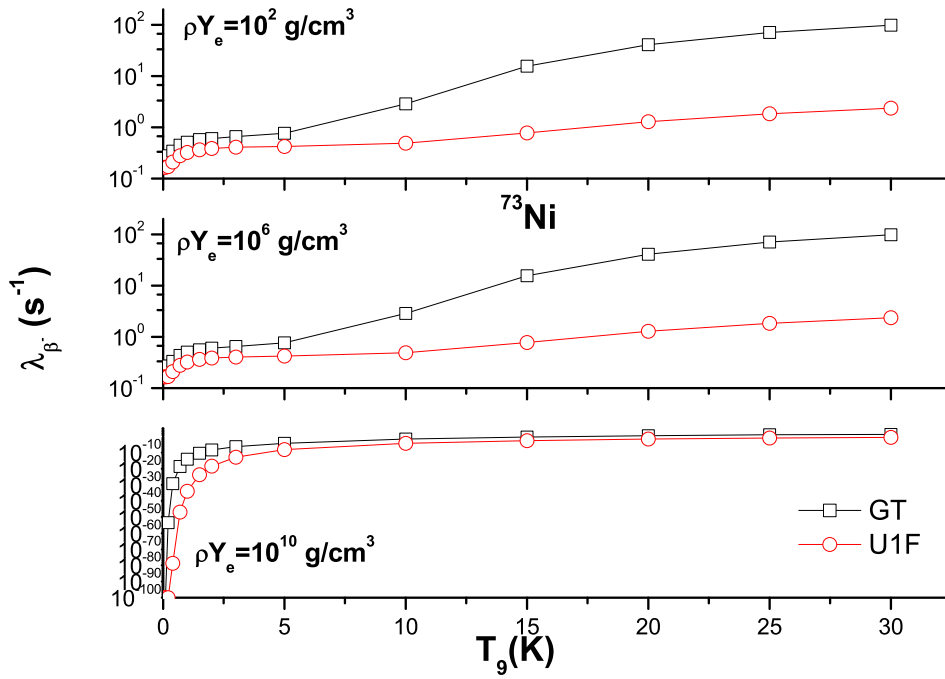


Fig. 5 Same as Fig. 4 but for ^{73}Ni .

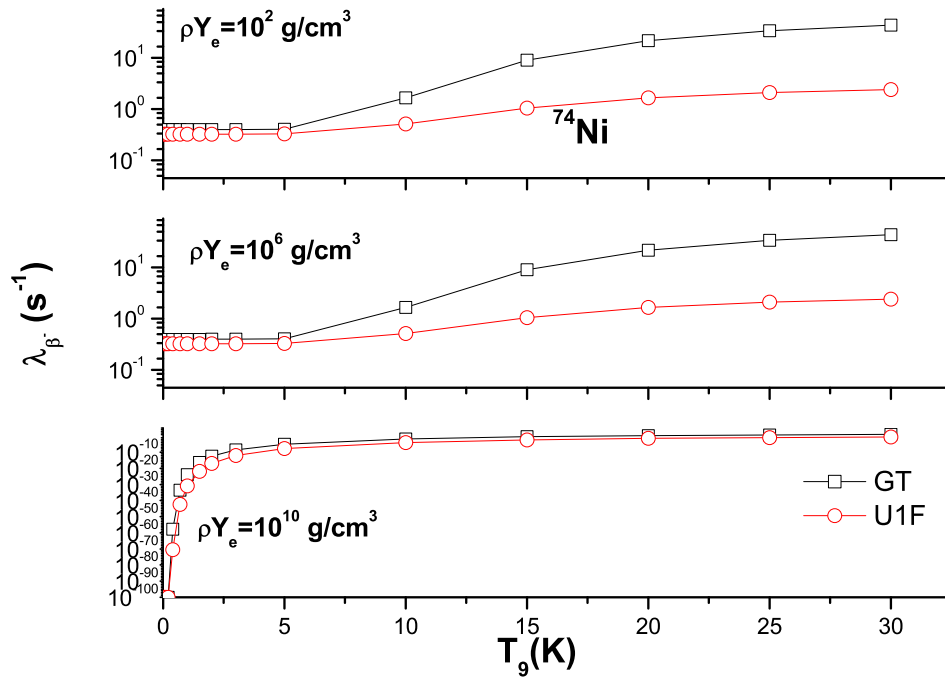


Fig. 6 Same as Fig. 4 but for ^{74}Ni .

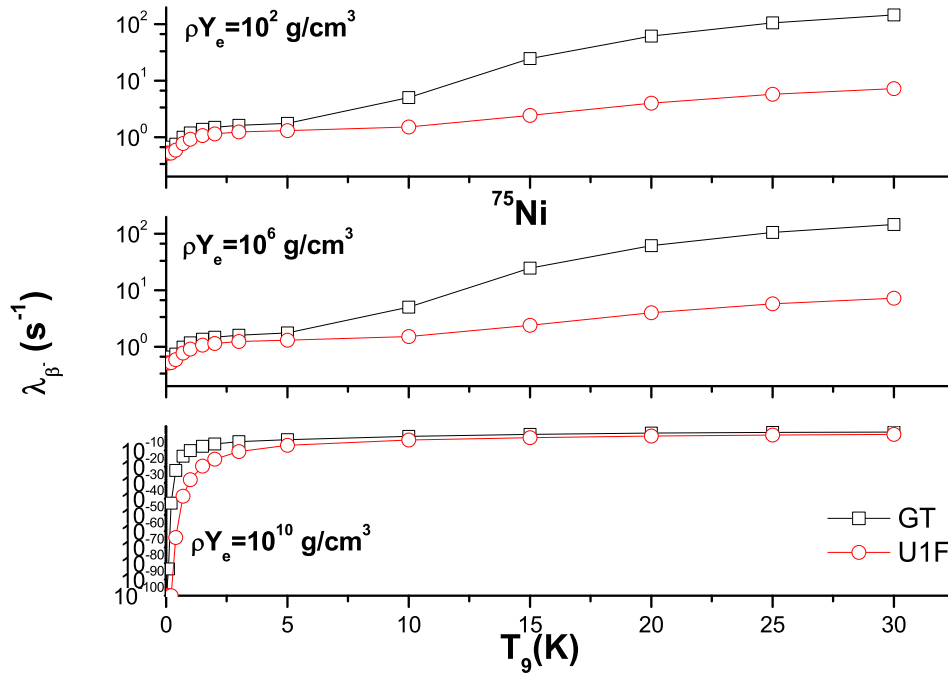


Fig. 7 Same as Fig. 4 but for ⁷⁵Ni.

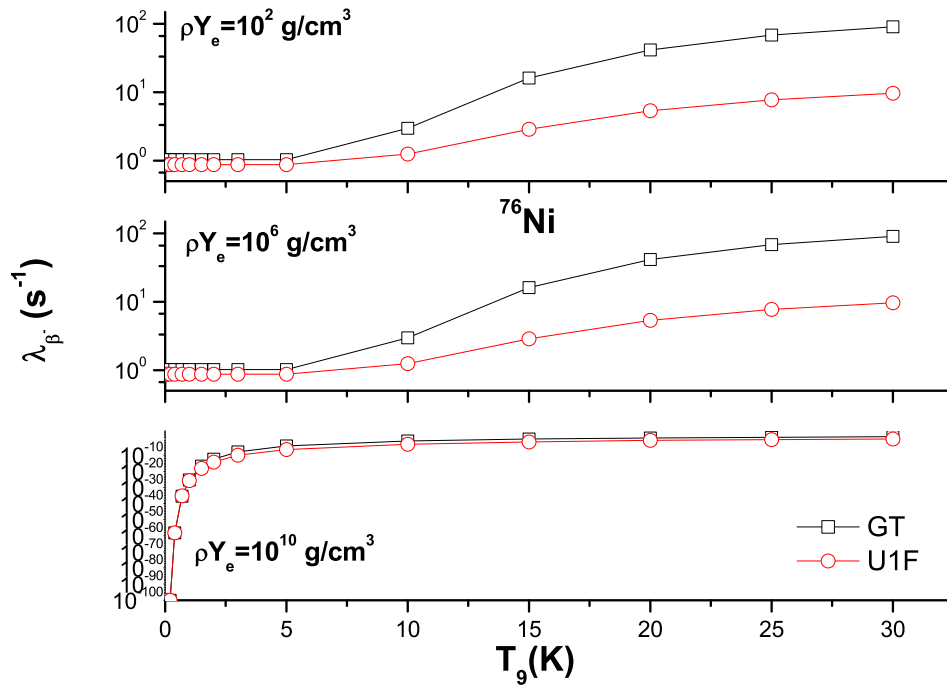


Fig. 8 Same as Fig. 4 but for ⁷⁶Ni.

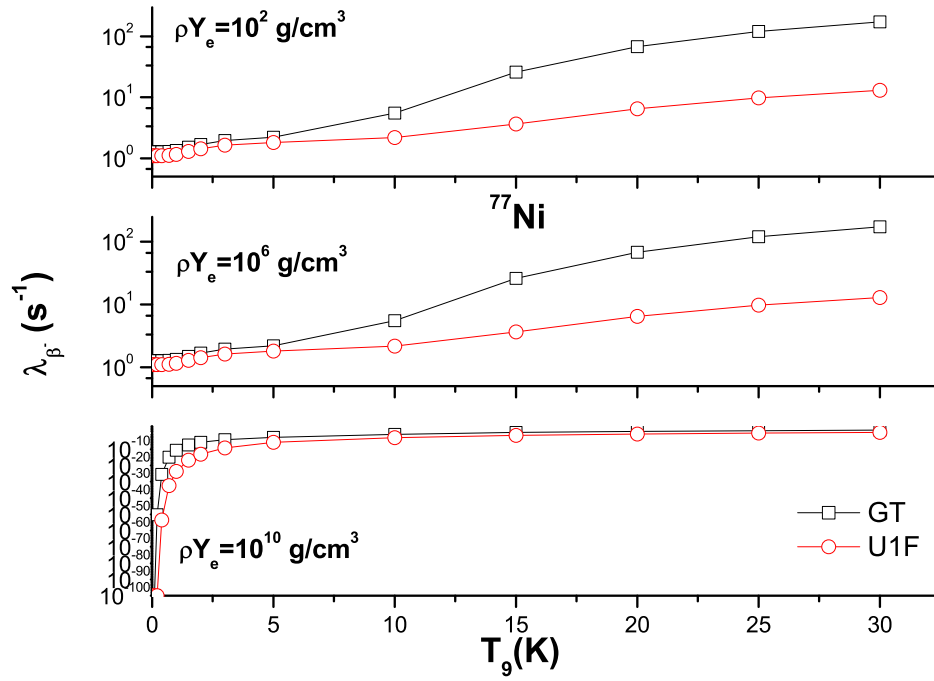


Fig. 9 Same as Fig. 4 but for ^{77}Ni .

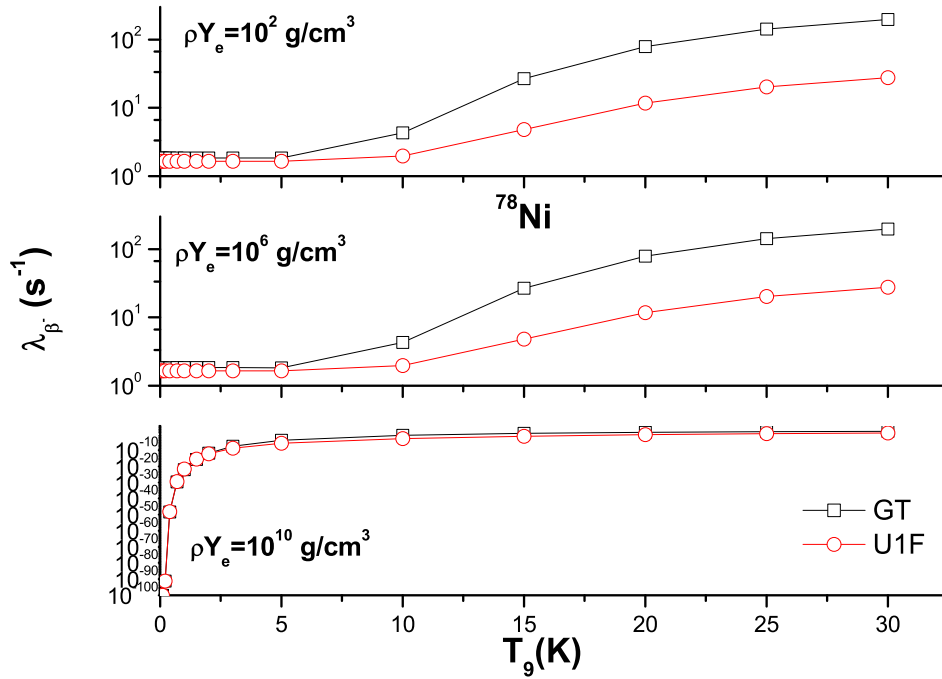


Fig. 10 Same as Fig. 4 but for ^{78}Ni .